Radiation Control in Deuterium, Tritium and Deuterium-Tritium JET baseline plasmas – part I

L. Piron [1,2], D. Van Eester[3], D. Frigione[4], L. Garzotti[5], P.J. Lomas[5], M. Lennholm[5], F. Rimini[5], F. Auriemma[2], M. Baruzzo[4] , P. J. Carvalho[6] , D.R. Ferreira[6] , A. R. Field[5] , K. Kirov[5], Z. Stancar[5] , C.I. Stuart[5] , D. Valcarcel[5] and the JET Contributors*

[1] *Dipartimento di Fisica "G. Galilei", Università degli Studi di Padova, Padova, Italy,*
[2] *Consorzio RFX, Corso Stati Uniti 4, 35127, Padova, Italy,*
[3] *Laboratory for Plasma Physics, LPP-ERK/KMS, Bruxelles BE*
[4] *ENEA, Fusion and Nuclear Safety Department, C.R. Frascati, Rome, Italy,*
[5] *CCFE, Culham Science Centre, Abingdon, OX14 3DB, United Kingdom,*
[6] *Instituto de Plasmas e Fusão Nuclear, Instituto Superior Técnico, Universidade de Lisboa, 1049-001, Lisboa, Portugal*

[(*)] *See the author list of "J. Mailloux et al 2022 Nucl. Fusion 62 042026 "*

The achievement of a steady ELMy H-mode phase with high ion temperature, but without a gradual rise in plasma radiation, has been a crucial point to establish high plasma performance scenarios in JET ITER-like-wall plasmas. Indeed, radiation events, due to the release of high Z impurities, such as Nickel and Copper, and W sputtered from the divertor, can strongly reduce the power crossing the plasma separatrix and slow the ELMs dynamics, thus inducing H to L transition. In particular, in JET baseline plasmas, because of the outward neoclassical transport [A.R. Field et al 2021 Plasma Phys. Control. Fusion 63 095013], plasma impurities are mainly localized in the mantle region, as detected by a real-time surrogate model for bolometer tomography based on machine learning [D.R. Ferreira et al 2021 Fusion Engineering and Design 164], and the consequent excessive radiation in this region is the main cause of plasma termination in recent Deuterium, Tritium and Deuterium-Tritium operations. To guarantee impurity accumulation being flushed by the ELMs, ELM control schemes, which ensure a throughput of particles, either via gas fueling and via pellets, have been exploited. In this work, the staged approach strategy towards radiation control, which allowed to sustain for more than 10 s Tritium and Deuterium-Tritium baseline discharges without radiation issues, is presented.

Keywords: JET, Plasma, Real-time control, DT, Tritium Operation, Radiation control, Plasma termination.

1. Introduction

In 2020/2021, JET offered the unique opportunity to study the behavior of Tritium (T) and Deuterium-Tritium (DT) plasmas in conditions and dimensions approaching those required in ITER (DTE2) [1]. With respect to the first DT campaign in 1997 (DTE1) [2], when JET was equipped with a Carbon wall, the experiments have been performed with a Tungsten (W) divertor and a Beryllium first wall, with an higher total auxiliary power and an improved coverage of diagnostics.

In preparation to DTE2, an intense activity of scenario development has been embarked in Deuterium to prepare the plasmas needed to demonstrate stationary high fusion performance [3] and a pure Tritium campaign has been conducted to assess how the isotopic effects affect the plasma scenarios developed, complementing the previous Hydrogen campaign studies [4] .

The main challenge that has been faced in JET with the new wall, if the frequency of ELMs (edge localized mode) become too low, is the risk of having plasmas polluted by high Z impurities, such as Nickel and Copper, and W sputtered from the divertor, which can cause radiation events, and thus plasma disruptions.

To avoid these events, low particle throughput has to be achieved by a proper control of ELM frequency. Over the years, various ELM control strategies have been developed and tested in JET baseline plasmas in preparation to DTE2 [5,6,7] which rely on i) vertical kicks, which consist in a rapid vertical plasma movement, by changing the radial magnetic field, ii) gas fuelling and iii) injection of pellets of frozen hydrogenic isotopes into the plasma.

Vertical kicks are not suitable for the high plasma current operations foreseen in DTE2 because of the associated risk of vertical displacement events. Gas flow alone is also not effective. High levels of gas are indeed requested to maintain ELM frequency as desired, which lead to plasma confinement degradation and hence performance reduction. The optimal ELM control strategy consists of using a combination of gas fuelling and ELM-pacing pellets. This is the control strategy adopted in T and DT baseline plasmas at Ip=3.5 MA, Bt= 3.25 T that are described in this paper.

The control of radiation has been challenging in T and DT. Indeed, the ELM frequency was lower in T than in D and the initial ELM-free phase was longer, as observed in DTE1 [8] and predicted by modelling [9].

author's email: lidia.piron@unipd.it

Hence, a staged approach has been adopted to identify the best settings of the ELM control actuators, i.e. gas flow and pellet injector, to guarantee an efficient flush of impurities from the plasma.

In this work, the path of radiation control in JET T and DT I_p=3.5 MA baseline plasmas is reported. In particular, Section 2 reports the lesson learn on radiation control from D operations. Section 3 summarizes the optimization of ELM control which allows to sustain a T and DT discharge with 33 MW auxiliary power (PNBI=29 MW+ PICRH =4MW) up to 50.2 s and 51 s, respectively, without radiation issue. Section 4 gives the conclusions.

2. Lesson learn from Deuterium operation

Excessive radiation has been the main cause of stop (e.g. the first event that triggers a controlled plasma termination) in JET D baseline plasmas, with a rate of 43%. Radiation runaway events are due the presence of high Z impurities and sputtered W from the divertor, which are not flushed out from the confined plasma but are mainly localized in the low-field side (LFS) region because of the outward neoclassical transport convention [10].

Radiation is monitored in JET by two systems:

i) the real-time control system, where several metrics are calculated by the Real Time Central Controller (RTCC), as the radiation fraction, which is the ratio between the total radiation as measured by the vertical bolometer fan [11] and the total input power, and bolometry peaking, defined as the ratio between a central and an off axis bolometer channel.

ii) the Plasma Event TRiggering for Alarm (PETRA) system [12], where a sophisticated tomographic bolometry algorithm based on machine-learning has been deployed [13] and offers the possibility of monitoring the radiated power in specific regions of interest, such as the LFS, where impurities tend to accumulate in baseline plasmas [9], and the core region, named here $P_{rad\ LFS}$ and $P_{rad\ core}$, respectively.

Since the plasma performance cannot recover from a radiation runaway event, as a radiation metrics exceeds a certain threshold, a controlled termination of the pulse, called jump to termination (JTT), is initiated.

To avoid a radiation collapse, it is of paramount importance to avoid heavy impurity accumulation. The experience that has been capitalized from D operation is that the combination of ELM pacing pellets + gas fuelling promotes the removal of impurities by means of ELMs.

This is demonstrated in Fig.1 which shows a pair of I_p=3.5 MA, B_t=3.25 T Deuterium discharges where two strategies for ELM control have been compared: only gas fuelling, in the pulse plotted in blue, pellets + gas fuelling, in the pulse in red. In particular, the train of ELM pacing

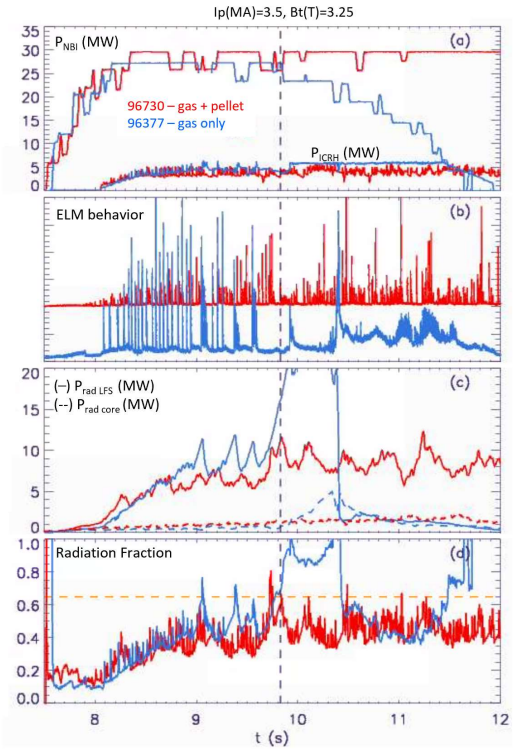

Fig.1. Time behavior of (a) auxiliary heating power, (b) ELMs, (c) radiation in the core (dotted line) and in the LFS (solid line) as calculated by bolometer tomography based on machine learning and (d) radiation fraction in a pair of I_p=3.5 MA, B_t=3.25 T Deuterium discharges. ELM dynamics is controlled by only gas fuelling in the discharge plotted in blue, while pellet+gas fuelling in the discharge in red. The vertical dotted line corresponds to the time instant of stop while the orange dotted line indicates the threshold on radiation fraction set in JET real-time control system.

pellets has been programmed at a repetition frequency of 45 Hz, in the time interval t=[7.55-8.5] s, then 35 Hz.

In the gas only fuelled pulse, as shown in Fig.1(b), after the L-H transition, regular type-I ELM can be observed, but from t=9 s, the ELMs are less reliably triggered, and there are periods of ELM free phases. This causes heavy impurities not being flushed anymore, until the 0.65 threshold on radiation fraction has been reached at around t=9.83 s, which initiates JTT. On the other hand, in the pellet + gas fuelled pulse, erratic type-I ELMs with a compound character have been triggered, which guaranteed a good flushing level of impurities and thus no radiation building up has been encountered through all the plasma phase.

It is worth mentioning that the pellet + gas fuelling recipe not only prevents radiation building up, but also corresponds to a lower total fuelling rate, part of the gas

fuelling being replaced with injection of pellet. This allows for a more modest deterioration of the confinement than with gas fuelling alone [3].

3. The path of radiation control in Tritium and Deuterium-Tritium

The experience gained from D operation suggested to use ELM-pacing pellets + gas fuelling to avoid radiation runaway events.

However, it has not been possible to apply straightforwardly such control scheme into T and DT plasmas because of isotope physics and operation related aspects. Indeed, in T and in DT, the dynamics of ELMs was slower than in D and the ELM free phase last longer. This was compounded by the different behavior of Tritium injection modules (TIMs) respect to gas injection modules (GIMs), and by the gas species itself. Therefore, the control of radiation has followed a staged approach, which envisaged the identification of the optimal settings in the pellet + gas fuelling scheme. It is worth highlighting that such an identification has been hampered by stringent limitations on experimental time available, on T consumption and neutron activation (in Deuterium-Tritium).

The path of radiation control is described in the following subsections, presenting baseline plasmas with 3.5 MA plasma current (I_p) and 3.25 toroidal magnetic field (B_t). In these experiments, the radiation level has been monitored continuously 0.5 s after the NBI injection, by a series of radiation metrics available in JET real-time control and PETRA systems.

3.1 Radiation control in Tritium

To guarantee flushing of impurities and thus avoiding radiation building up, gas fuelling and pellet injector settings have to be tuned when operating in Tritium.

The level of gas flow has been chosen, based on the response of GIMs [7], to achieve a density level, and thus an H mode entry, similar to the D one. Regarding the injection of pellets, 2 mm Hydrogen pellets have been lanced from a flight line located at the upper high-field side of the main vessel [12]. The pellet injection time and frequency have been scanned with the aim of delaying the radiation building up.

In first T baseline attempt at I_p=3.5 MA, reported in blue in Fig.2, Hydrogen pellets at 25 Hz requested frequency has been injected from t=8.5 s. The plasma transited in H mode at around t=7.75 s, as shown in Fig.2 (b), but ELMs have been sporadically triggered. This induced radiation runaway which was localized in the LFS, as indicated by the real-time tomographic bolometry metrics, reported in Fig.2 (c) with a solid line. After the long ELM-free phase of duration ~0.2 s, the radiation power increased to more than 60% of the input power, as shown in Fig.2 (d), at which point this triggered a controlled termination of the pulse, which commenced with a strong increase of the gas puffing rate (not shown).

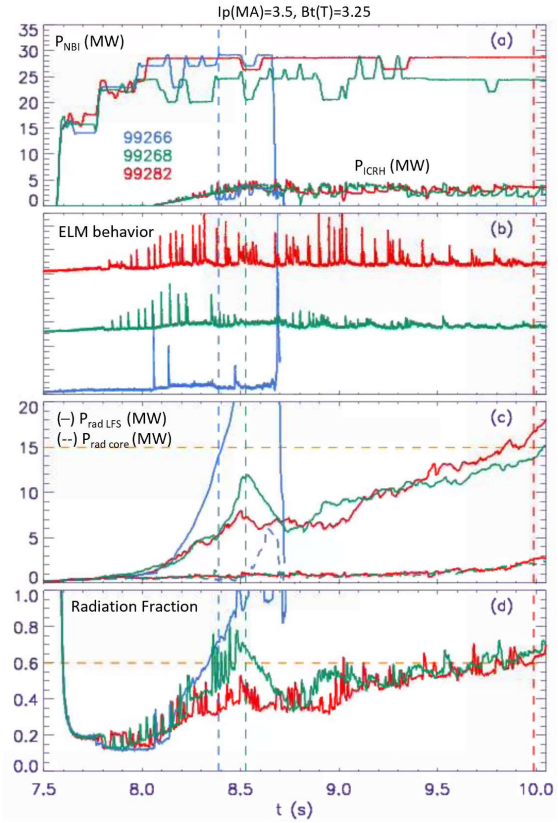

Fig. 2. Time behavior of (a) auxiliary heating power, (b) ELMs, (c) radiation in the core (dotted line) and in the LFS (solid line) as calculated by bolometer tomography based on machine learning and (d) radiation fraction in three I_p=3.5 MA, B_t=3.25 T Tritium discharges, which differ from pellet injection settings. The time of the stop is highlighted with a dotted line.

To promote ELM triggering, the injection of pellets has been thus anticipated to t=7.55 s in the pulse plotted in green in the same figure. In this case, after the H mode entry, at around t=7.8 s, regular ELMs paced at 25 Hz have been triggered, as reported in Fig.2 (b). However, an ELM free phase occurred, which was responsible of impurity accumulation, mainly in the LFS, and thus radiation building up. Similarly to the previous discharge, but with a 0.140 s delay, JET real-time control system detected an excessive radiation fraction level in the plasma, above 60%, and initiated the pulse termination.

To prevent ELM free phases, the pellet injection rate has been increased from 25 Hz to 35 Hz in the time interval t=[7.55- 8.75] s, and afterwards has been set at 17 Hz. These settings have been tested in the plasma plotted in red in Fig.2. As shown in Fig.2(b), these settings ameliorate the ELM dynamics resulting in higher frequency, higher amplitude ELMs which allowed to delay the radiation building up of t=1.5 s w.r.t. the previously described discharge. However, at around t=10 s, the empirically identified 15 MW threshold was

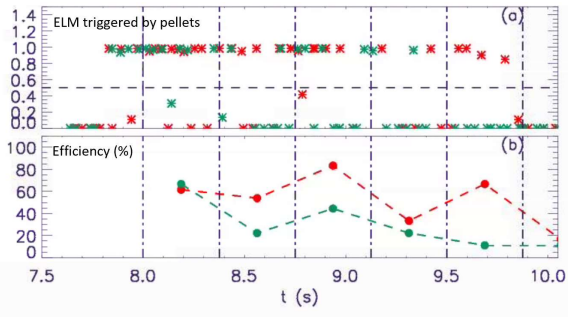

Fig. 3.Time behavior of (a) the probability of an ELM being triggered by a pellet [12] and (b) pellet efficiency in triggering an ELM. Data corresponds to the set of discharges presented in Fig.2.

reached by the $P_{rad\ LFS}$ metrics, as detected by PETRA system, which commenced the plasma termination.

The ELM control settings using in this discharge are the optimal ones at present since they allowed to maintain radiation under control in a I_p=3.5 MA baseline plasmas with 33 MW input power up to t=10.2 s.

It is worth highlighting that not all the injected pellets triggered ELMs. This has been quantified by calculating the efficiency indicator which is the ratio between the probability of an ELM being triggered by a pellet, based on a Bayesian approach described in [14], and the number of pellet injected within a time interval. The results of this analysis is shown in Fig.3. The time intervals where the analysis has been carried out are represented with a dotted vertical line in the figure. Note that overall, the pellet injection settings used in the discharge plotted in red in Fig.2 resulted in a efficiency level on average above 50%, larger w.r.t the one in the pulse in green. Indeed, these optimal settings have guaranteed a good impurity flushing, delaying the radiation building up.

3.2 Radiation control in Deuterium-Tritium

Radiation control in DT operation, analogously to T operation, has followed a staged approach. In particular, a scan of pellet frequency and a scan of gas fuelling have been performed to identify the optimal settings in the ELM control actuators which can prevent impurity accumulation and thus the radiation collapse.

Fig.4 presents a series of DT discharges at I_p=3.5 MA, B_t=3.25 T where the gas flow has been tuned to achieve a density level at H mode entry similar to the D one and then has been set around 1 x10^{22} (e/s) in the main heating phase. The frequency of D pellet injection has been varied in these discharges: in the pulse plotted in green, the pellets have been injected from t=7.55s at 45 Hz, in the pulse plotted in blue, the same settings have been used up to t=8.5 s, but then, the pellet frequency has been reduced at 35 Hz. In the pulse plotted in red, because of the malfunction in the pellet injection, no pellets have been delivered to the plasma, so it can be counted as only gas fuelled pulse. This discharge is of particular interest because it shows the importance of a reliable pellet injection to avoid radiation runaway events. Indeed, without pellet injection, ELMs were sporadically triggered and interval of ELM free phases occurred, which favored impurity accumulation and thus an exponential increase of radiation, which was detected at around t=8.5 s as the radiation fraction metrics reached the 80% level.

On the other hand, in both the pulse with pellets successfully injected, as shown in Fig.4(b), ELMs exhibited a complex behavior, with some large, type-I ELMs, each followed by a period of small ELMs before t=10 s. The efficiency of pellet in triggering an ELM was in both the cases above 60% (not shown). However, after t=10 s, the ELM bursts have smaller amplitude and the pellet' efficiency starts to decrease. Consequently, the radiation increased and a stop due to excessive radiation fraction, in the pulse plotted in blue, and excessive Prad in the LFS, in the plasma in green, have been detected by JET real-time control system and PETRA system, respectively. This happened around t=10.6 s, in both the cases.

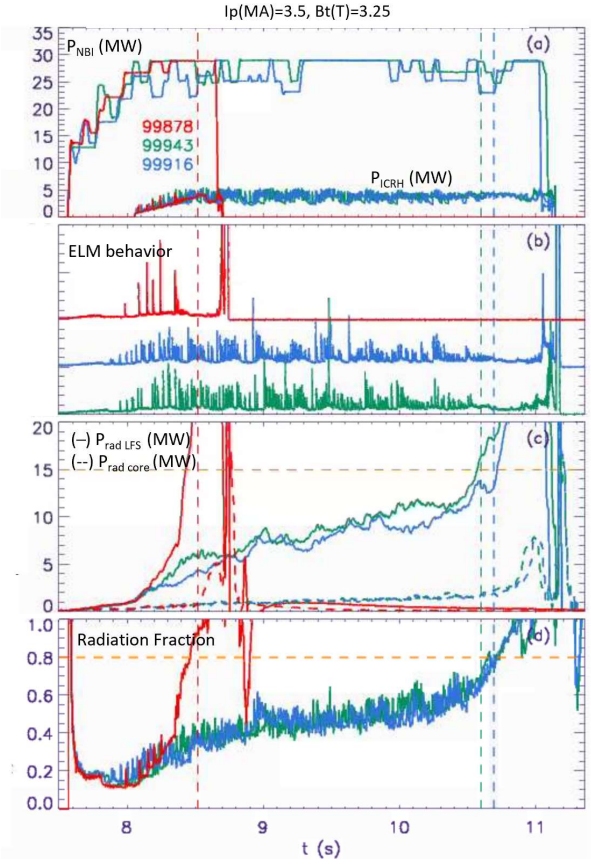

Fig. 4. Time behavior of (a) auxiliary heating power, (b) ELMs, (c) radiation in the core (dotted line) and in the LFS (solid line) as calculated by bolometer tomography based on machine learning and (d) radiation fraction in three of I_p=3.5 MA, B_t=3.25 T Deuterium-Tritium discharges, which differ from pellet injection frequency. The time of the stop is highlighted with a dotted line.

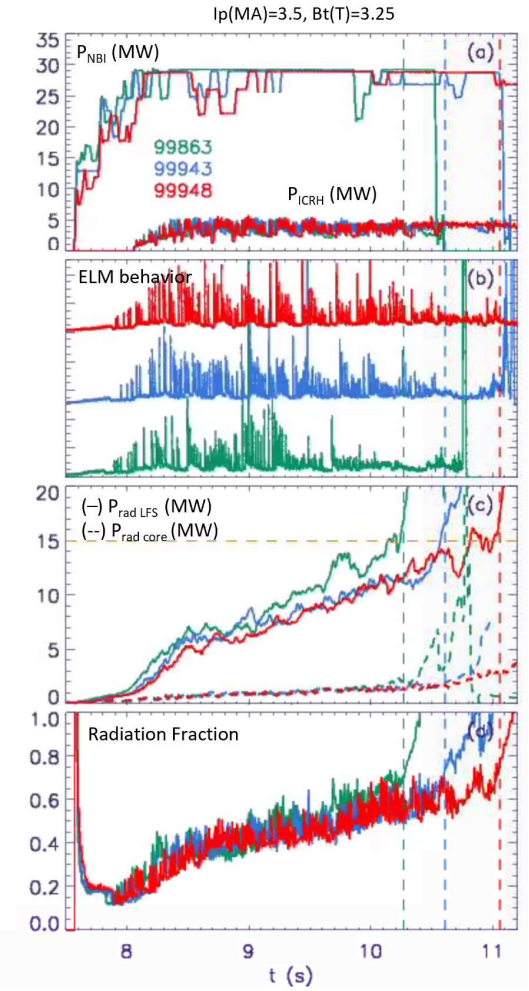

Fig. 5. Time behavior of (a) auxiliary heating power, (b) ELMs, (c) radiation in the core (dotted line) and in the LFS (solid line) as calculated by bolometer tomography based on machine learning and (d) radiation fraction in three I_p=3.5 MA, B_t=3.25 T Deuterium-Tritium discharges, which differ from the gas fuelling rate. The gas fuelling rate used is described in the text. The time of stop is highlighted with a dotted line.

The similar behavior of radiation dynamics in these discharges suggests that the change of pellet frequency from 35 Hz to 45 Hz did not improve radiation control. This insight is also confirmed by a statistical analyses performed for the all DT database reported in [15].

As aforementioned, a gas fuelling scan has been also carried out in DT plasmas, while keeping the same 45 Hz pellet frequency from t=8.5 s, to assess its role in delaying the radiation building up.

The results of such a gas scan, which has been performed from t=9 s, are reported in Fig.5. A colour code has been used here to distinguish the various gas flow levels (green corresponds to the lower gas rate, indicatively about 0.7 x10^{22} (e/s), blue to the medium gas rate, about 1 x10^{22} (e/s), and red to the higher gas rate, about 1.5 x10^{22} (e/s)). The radiation, as shown in Fig.5(c-d), slowly increased in time, up to a point in which the 15 MW threshold set in PETRA on the $P_{rad\ LFS}$, has been

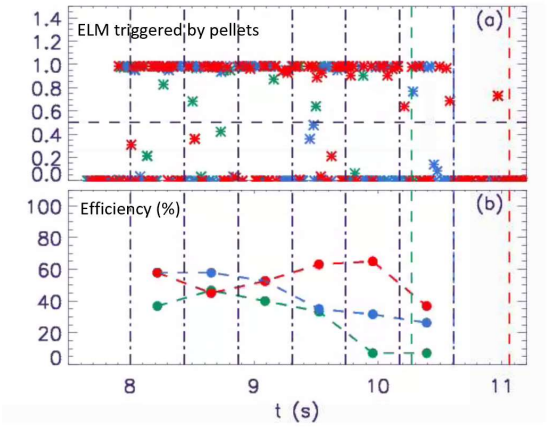

Fig. 6. Time behavior of (a) the probability of an ELM being triggered by a pellet [12] and (b) pellet efficiency in triggering an ELM. Data corresponds to the set of discharges presented in Fig.5.

reached. Note that such a threshold was achieved later on as the gas flow level was increased. Actually, in the pulse plotted in red, the radiation has been maintained controlled up to t=11 s. This implies that the optimal gas fuelling rate is around 1.5 x10^{22} (e/s), based on the present knowledge.

The discharge where this gas fuelling rate has been tested had also a larger chance of having an ELM being triggered by a pellet. This is shown in Fig.6 (b) where the calculation of pellet's efficiency in triggering ELMs is reported for the discharges with different gas flow rates.

4. Conclusion

This work summarized the main achievements obtained on radiation control during T and DT experiments in JET which took place in 2020/2021.

To monitor radiation evolution, a series of metrics were available in real-time, which have been calculated by programmable schemes using bolometric signals in the JET real-time control system, and derived by a surrogate model for bolometer tomography, based on machine learning, available in the brand-new PETRA system.

In DT and especially in T, the control of radiation per se has been challenging because of the different ELM dynamics with respect to D operation, the different behavior of gas GIMs w.r.t. TIMs and the gas species itself used. This has been also acerbated by the limited experimental time available and the restrictions imposed by T consumption and neutron activation (in DT).

In this context, a staged approach has been pursued to identify the optimal settings of gas dosing and pellet injection, which promote an efficient impurity flushing by means of ELMs, while guarantying good plasma confinement properties.

The optimal settings for ELM control allow to sustain I_p=3.5 MA, B_t=3.35 T baseline T and DT discharges up to 10.2 s and 11 s, respectively, without radiation issues. Generally, the operation in T pulse suffers from high level of radiation, and hence, high impurity content. This can be due to different mechanisms, such as the increased sputtering due to the higher isotope mass [16], the development of hollow density profiles which can affect plasma transport [15] and different power threshold for the L to H transition in these plasmas. The properties of the radiated power in T and DT plasma are still under investigation, and once a deep knowledge will be acquired, a further optimization of control schemes for radiation control will be carried out in preparation to DTE3 campaign.

Acknowledgments

This work has been carried out within the framework of the EUROfusion Consortium, funded by the European Union via the Euratom Research and Training Programme (Grant Agreement No 101052200 EUROfusion). Views and opinions expressed are however those of the author(s) only and do not necessarily reflect those of the European Union or the European Commission. Neither the European Union nor the European Commission can be held responsible for them. As shown here: https://users.euro-fusion.org/publications/fp9/.

References

[1] J. Mailloux et al 2022 Nucl. Fusion 62 042026

[2] M. Keilhacker et al 1999 Nucl. Fusion 39 209

[3] L. Garzotti et al 2019 Nucl. Fusion 59 076037

[4] C.F. Maggi et al 2018 Plasma Phys. Control. Fusion 60 014045

[5] F.G. Rimini et al 2011 Fusion Eng. and Design 86 539-543

[6] M. Lennholm et al 2015 Nucl. Fusion 55 06300

[7] L. Piron et al 2021 Fusion Eng. and Design 166 112305

[8] JET Team 1999 Nucl. Fusion 39 1875

[9] S.E. Snyder et al 2005 Physics of Plasmas 12 112508

[10] A.R. Field et al 2021 Plasma Phys. Control. Fusion 63 095013

[11] A. Huber et al 2007 Journal of Nuclear Materials 363–365 365-370

[12] C.I. Stuart et al 2021 Fusion Engineering and Design 168 112412

[13] D.R. Ferreira et al 2021 Fusion Engineering and Design 164 112179

[14] M. Lennholm et al 2021 Nucl. Fusion 61 036035

[15] L. Piron et al statistics of radiation control in D,T,DT plasmas, paper in preparation

[16] C. Guillemaut et al 2016 Phys. Scr. T167 014005